Journal of
Composites Science

MDPI

Article

Mechanical, Durability, and Microstructure Characterization of Pervious Concrete Incorporating Polypropylene Fibers and Fly Ash/Silica Fume

Hassan Bilal [1], Xiaojian Gao [2], Liborio Cavaleri [1,*], Alamgir Khan [2] and Miao Ren [3]

[1] Department of Engineering, University of Palermo, Viale Delle Scienze, 90128 Palermo, Italy; hassan.bilal@unipa.it
[2] School of Civil Engineering, Harbin Institute of Technology, Harbin 150090, China; gaoxj@hit.edu.cn (X.G.); alamgirkhan@stu.hit.edu.cn (A.K.)
[3] Department of Civil and Environmental Engineering, The Hong Kong Polytechnic University, Hong Kong 999077, China; miaoren@polyu.edu.hk
* Correspondence: liborio.cavaleri@unipa.it; Tel.: +39-091-23896733

Abstract: Pervious concrete, because of its high porosity, is a suitable material for reducing the effects of water precipitations and is primarily utilized in road pavements. In this study, the effects of binder-to-aggregate (B/A) ratios, as well as mineral admixtures with and without polypropylene fibers (PPFs) (0.2% by volume), including fly ash (FA) or silica fume (SF) (10% by substitution of cement), on the mechanical properties and durability of pervious concrete were experimentally observed. The experimental campaign included the following tests: permeability, porosity, compressive strength, splitting tensile strength, and flexural strength tests. The durability performance was evaluated by observing freeze–thaw cycles and abrasion resistance after 28 d curing. X-ray diffraction (XRD), Fourier transform infrared spectroscopy (FTIR), thermal analysis (TGA-DTA), and scanning electron microscopy (SEM) combined with energy dispersive spectroscopy (EDS) were employed to investigate the phase composition and microstructure. The results revealed that, for an assigned B/A ratio identified as optimal, the incorporation of mineral admixtures and fibers mutually compensated for their respective negative effects, resulting in the effective enhancement of both mechanical/microstructural characteristics and durability properties. In general, pervious concrete developed with fly ash or silica fume achieved higher compressive strength (>35 MPA) and permeability of 4 mm/s, whereas the binary combination of fly ash or silica fume with 0.2% PPFs yielded a flexural strength greater than 6 MPA and a permeability of 6 mm/s. Silica fume-based pervious concrete exhibited excellent performance in terms of freeze–thaw (F-T) cycling and abrasion resistance, followed by fiber-reinforced pervious concrete, except fly ash-based pervious concrete. Microstructural analysis showed that the inclusion of fly ash or silica fume reduced the harmful capillary pores and refined the pore enlargement caused by PPFs in the cement interface matrix through micro-filling and a pozzolanic reaction, leading to improved mechanical and durability characteristics of pervious concrete.

Keywords: pervious concrete; polypropylene fibers; fly ash/silica fume; mechanical properties; durability; microstructure

Citation: Bilal, H.; Gao, X.; Cavaleri, L.; Khan, A.; Ren, M. Mechanical, Durability, and Microstructure Characterization of Pervious Concrete Incorporating Polypropylene Fibers and Fly Ash/Silica Fume. *J. Compos. Sci.* **2024**, *8*, 456. https://doi.org/10.3390/jcs8110456

Academic Editors: Xiangfa Wu and Oksana Zholobko

Received: 16 September 2024
Revised: 18 October 2024
Accepted: 27 October 2024
Published: 3 November 2024

1. Introduction

Pervious concrete has gained advantages over dense-graded asphalt and Portland cement concrete pavement materials due to its multifold benefits provided by the interconnected network of macropores, which mitigates the negative impact of urban flooding and enhances the sound absorption properties [1–3]. Water infiltration through an interconnected network of voids can also improve the evaporative cooling effect [4]. Considering the prominent environmental benefits and better hydrological performance of pervious

concrete pavements, the concept of a sponge city has been launched to pursue feasible and viable solutions to address urban flood problems, urban sustainability, water conservation, and water quality issues in urban areas [5,6].

Numerous uncertainties and challenges associated with pervious concrete design, practical implementation, and modeling must be comprehensively deepened [7–11]. From the material procurement and mix design perspectives, different parameters influencing load-carrying capacity, water permeability, and durability performance are of fundamental importance. The interconnected voids in porous concrete, which are potentially favorable for water infiltration, can negatively influence compressive strength, abrasion resistance, and durability performance [12,13]. To overcome the issue of lower mechanical and durability performance, various possible industrial by-products, such as silica fume, fly ash, metakaolin, ground blast furnace slag, steel slag, and polymers, for instance, polypropylene fibers and styrene butadiene rubber, have been added to the mix design [14–21]. Recently, the incorporation of various recycled aggregates, waste tire rubber, palm oil clinker, and crushed seashells as coarse aggregates in pervious concrete fabrication has attracted significant attention. However, these recycled materials generally have undesirable effects on mechanical properties and durability [22–25]. To compensate for the performance loss due to these low-quality recycled materials, the substitution of cement with various industrial by-products has been recommended [26,27].

According to Lian and Zhuge [28], the parameters influencing the mechanical strength and porosity of pervious concrete are the cement content, binder-to-aggregate ratio (B/A), water-to-cement ratio (W/C), and gradation method. Zhong and Wille [29] reported a reduced compressive strength with an increased aggregate size and aggregate-to-binder ratio (A/B). Similar conclusions have been achieved in [30]. In the study of Yang and Jiang [31], the vibration molding method and the use of a medium aggregate size have been proposed as favorable for achieving optimum mechanical and permeability performance. In the study of Kevern et al. [32], the use of smaller coarse aggregates and silica fume (SF) for partial cement replacement, along with the addition of superplasticizer, resulted in a considerable increase in the compressive strength and flexural strength, with excellent freeze–thaw durability. Kevern et al. [32] found that substituting a portion of fine sand with coarse aggregate and polypropylene fibers within a certain dosage demonstrated good resistance to rapid freeze–thaw cycling and better mechanical strength with good permeability. The performance of short fibers was better than that of long fibers because of the uniform distribution and interweaving among them, resulting in a greater coverage of aggregates.

The strength of pervious concrete is strongly associated with the bonding strength between aggregate particles and the strength of the cement paste layer. The intra-bonding among particles can be improved by using graded coarse aggregates, whereas a greater cement paste thickness can be achieved by incorporating inert fillers and pozzolanic admixtures (silica fume or fly ash) with physical fibers. The inert materials produce a filler effect, whereas the pozzolanic admixtures produce both filler and chemical effects [21,27]. Huang et al. [33] examined the impact of aggregate size and mineral admixtures, including silica fume and fly ash, on the strength and permeability of pervious concrete at various W/C ratios based on 18% optimum porosity. Their findings revealed that an optimal content of 6% silica fume and 10% fly ash by weight replacement with cement could allow a considerable compressive strength and permeability to be achieved. Saboo et al. [34] also reported the dominant effect of a fly ash content ranging from 5 to 15% with 2% metakaolin on the permeability and compressive strength of pervious concrete. Wang et al. [35] investigated the influence of the binder/aggregate ratio (B/A) and the amount of fly ash on the porosity and compressive strength of pervious concrete and recommended an optimum B/A of 0.20–0.24 and 20% fly ash content to produce high-strength pervious concrete. In addition, the biotoxicity of percolates has been evaluated for runoff pollution control and rainwater recycling. Both studies [34,35] recommended further research on the durability of pervious concrete based on the optimum binder/aggregate ratio. Nazeer

et al. [36] also reported significant improvement in pervious concrete strength, abrasion, and acid resistance with 10% fly ash (FA) and silica fume. Further, Kevern et al. [37] confirmed the results in [32].

According to the literature, the incorporation of fiber may significantly influence the mechanical properties, permeability, and durability of pervious concrete. Dai et al. [27] reported the single- and multi-modified effects of physical fibers (0.2–1.2% polypropylene fiber and 2% basalt fiber) and mineral admixtures (15% fly ash and 6% silica fume of the cement as substitution) on the compressive strength, permeability, and porosity. The multi-modification effect of physical fibers on the strength characteristics was better than that of mineral admixtures without fibers. In contrast, in [37,38], only improved mechanical and permeability properties due to enhanced void connectivity were found after fiber inclusion. It has also been found in [32] that longer fibers can offer better freeze–thaw performance and lower permeability but no significant impact on the compressive strength.

On the other hand, Wu et al. [39] observed that polypropylene fiber substantially increased the tensile strength and freeze–thaw durability. Singh et al. [40] also observed that 12 mm polypropylene fibers (PPFs) with a 0.4% volume fraction in pervious concrete improved the flexural and split tensile strength but had no significant effect on compressive strength, porosity, and permeability. In contrast, Juradin et al. [41] observed that the inclusion of 10 mm PPFs at a volume fraction of 0.18% had a negative effect on the porosity and permeability but improved the mechanical properties with the vibration compaction method. Ozel et al. [42] found an increase in porosity, permeability, and displacement but no remarkable improvement in strength at a 0.5% volume fraction of PPFs in pervious concrete. In [43], to improve the fiber–matrix interface bonding, polypropylene fibers were treated by chemical modification, resulting in a 10% increase in flexural strength compared to untreated fibers in pervious concrete. Wu et al. [44] studied the effect of PPF content (3, 6, and 9 kg/m^3) with 25% silica fume on the physical and mechanical characteristics of pervious concrete. Their results showed that the strength increased with the fiber content but the porosity and permeability decreased.

These studies, sometimes diverging in the results, highlight the need for further investigation of the combined influence of PPFs and supplementary cementitious materials on the characteristics of pervious concrete to provide a more comprehensive examination of the PPF-dependent mechanisms. Hence, this paper, after highlighting the need for further investigation of the combined influence of polypropylene fibers and supplementary cementitious materials on the characteristics of pervious concrete, focuses just on this issue of trying to observe the main mechanical and physical characteristics gained (or lost) by pervious concrete thanks to the above-mentioned additional components.

Based on a literature review, current research on fiber-reinforced pervious concrete has been, therefore, primarily focused on its physical and mechanical properties, with limited attention given to its durability performance. Therefore, here, the optimum binder-to-aggregate (B/A) ratio that would result in a good compressive strength while maintaining adequate permeability and porosity has been evaluated by experimental observations. Then, mineral admixtures, including fly ash and silica fume, were used to partially replace cement, and the combined effects of fly ash and silica fume with polypropylene fibers at the optimum B/A ratio were investigated to assess the mechanical characteristics and durability performance of pervious concrete. Finally, a microstructural characterization was performed to examine the impact of PPFs and mineral admixtures on the microstructure of pervious concrete.

2. Materials and Methods

2.1. Raw Materials

Portland cement, with a 42.5-grade strength, was used. The silica fume used in this study had a spherical particle size of less than 1 μm and a specific surface area of 17.30 m^2/g, e.g., [45]. Polycarboxylate as a superplasticizer (SP) was adopted by trial and error based on trial batch mixes to adjust the workability of the pervious concrete. Class II fly ash was

used in accordance with Chinese Standard GB/T50146-2014, e.g., [46]. Polypropylene fibers with a length of 9 mm, a density of 0.9 g/cm^3, a diameter of 18–48 micro-micrometers, a tensile strength of 458 MPa, and an elastic modulus of 3.5 GPa were employed to obtain an anti-cracking effect. Table 1 lists the chemical compositions of the raw materials as determined by X-ray fluorescence (XRF) spectrometry.

Table 1. The chemical composition of raw materials (wt %).

Chemical Composition Index (%)	CaO	SiO_2	Al_2O_3	SO_3	MgO	Fe_2O_3	Loss on Ignition
Cement (OPC)	63.25	20.38	4.26	4.10	3.08	3.58	2.97
Silica fume (SF)	0.64	87.67	0.28	0.82	1.80	0.60	1.57
Fly ash (FA)	11.53	56.16	17.33	0.49	1.13	9.47	3.00

2.2. Mixing of Polypropylene Fibers with Raw Materials

The PPFs were manually mixed with 5% cement and fine sand before being added to the mechanical mixer. The addition amount was generally not more than 0.20% by concrete volume owing to the agglomeration and non-uniform distribution of fibers. After proper mixing, no lumps or agglomerations of polypropylene fibers were observed during the mixing process. Then, a mixture of cement, fine sand, and fibers was added to the aggregate, which had already been mixed with 5% cement, to coat the surface of the aggregates. This mixing method was adopted to improve the bonding of the cement paste with coarse aggregates. The mixing time was increased with respect to the standard mixing to uniformly distribute the polypropylene fibers in the mix, firmly holding and wrapping around the aggregates. It was observed that adding polypropylene fibers increased the workability and cohesiveness of the fresh mix. Prolonged mixing did not affect the fiber distribution and strength and did not cause agglomeration. Silica fume and fly ash were also properly mixed with PPFs under dry conditions before being added to the mixer. This mixing method effectively distributed the fibers in the fresh concrete mixture and increased the homogeneity of fibers. All mixing operations were performed in a mechanical drum mixer with sufficient mixing power and capacity to properly mix and produce a workable mixture.

2.3. Mix Proportions and Specimen Preparation

The mix proportions of pervious concrete designed to partially replace cement with silica fume and fly ash are presented in Table 2. All mixes included fine sand 5% by weight of the coarse aggregate (4.75~9.5 mm). Fly ash and silica fume (Figure 1) replaced cement at 10% by weight; this 10% substitution ratio of fly ash and silica fume was found to be optimum for balancing the mechanical and functional properties of pervious concrete. This finding agrees with several literature studies [15,22,34,35,37]. Various mixes were fabricated to assess the influence of small coarse aggregate (4.75–9.50 mm) and various binder-to-aggregate (B/A) ratios on the compressive strength and water permeability properties of pervious concrete. In the reference mix with only polypropylene fibers, as mentioned before, 0.20% by concrete volume was used. The combined effects of fly ash (FA, 10%) and silica fume (SF, 10%) with polypropylene fibers (PPFs, 0.20% vol) at the optimum B/A ratio were then considered to assess the mechanical characteristics and durability performance of pervious concrete.

Table 2. Mix design for pervious concrete, kg/m^3.

Specimens' Nomenclature	Cement	Coarse Aggregate	Sand (5 wt.% of Coarse Aggregate)	FA (10 wt.% Replacement of Cement)	SF (10 wt.% Replacement of Cement)	PPFs (0.2% by Volume)	Water (W/C by Weight = 0.28)	SP (1.25 wt.% of Binder)
PC1-FA	315	1504	75.2	35	-	-	98	4.375
PC2-FAP	315	1504	75.2	35	-	1.8	98	4.375
PC3-SF	315	1504	75.2	-	35	-	98	4.375
PC4-SFP	315	1504	75.2	-	35	1.8	98	4.375
PC5-PP-Rf	350	1504	75.2	-	-	1.8	98	4.375

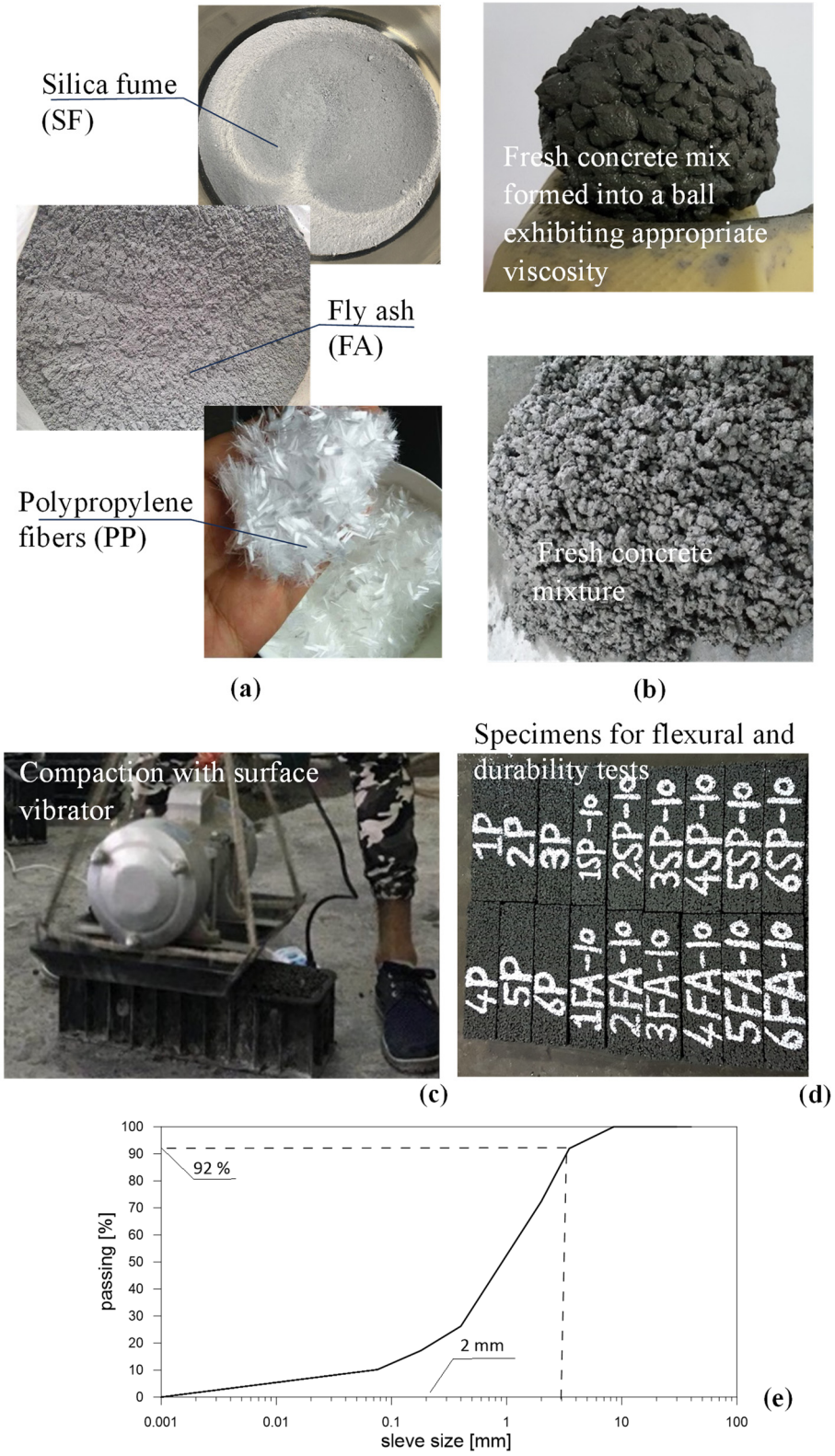

Figure 1. Raw materials (**a**), mixture consistency (**b**), compaction of fresh pervious concrete (**c**), specimens (**d**), and sand grading curve (**e**).

The cube specimens (100 mm × 100 mm × 100 mm) were manufactured in three lifts, each tamped 25 times. The mold was filled with fresh concrete in the third lift, and the extra concrete was struck off using a square trowel. Subsequently, the specimens were placed on plain hard ground, and each mold was vibrated for 30 s using a surface vibrator to

simulate field conditions. After compaction, all the samples were covered with a polythene plastic film and kept at room temperature for 24 h. Beam specimens with dimensions of 100 mm × 100 mm × 400 mm were cast for flexural and durability tests. Also, cylinders (diameter 100 mm and height 200 mm) were cast for splitting tests. The compaction was applied for 30 s using a surface vibrator. The vibration method is also regarded as the optimal method for producing pervious concrete with uniform air void distribution and superior void characteristics. All cube, cylinder, and beam specimens were demolded after 24 h. Water was sprayed onto the specimens to keep them moist, and they were stored in a standard curing room until the designated testing day. Binder cement paste specimens of 50 mm × 50 mm × 50 mm cubes were also prepared, corresponding to pervious concrete mixes. The curing conditions of the binder cement pastes were consistent with those of the pervious concrete. A mix design with an appropriate water content would neither collapse the internal channel of voids nor lead to cement segregation and permeability reduction. The fresh mix was formed into a ball, as shown in Figure 1b, firmly bonding the cement paste and aggregates together without crumbling and collapsing into pieces. The fresh workability of the mix determines the porosity and quality of the hardened pervious concrete. Figure 1 illustrates the raw materials, fresh concrete mix consistency assessment, placement and fabrication, and vibration of pervious concrete.

2.4. Testing Methods

2.4.1. Mechanical Testing

Compressive strength tests were carried out after 7, 14, 28, and 90 days of curing. Splitting tensile and flexural strength tests were also conducted after 28 days of curing as outlined in GB/T50081-2002 [47]. The average value of triplicate specimens was presented as the strength value at the defined curing age. Mechanical testing provides information on the bulk strength of the evaluated pervious concrete and critical insight into the qualitative relationship between the strength and the desired characteristics.

2.4.2. Permeability Test

The permeability of pervious concrete was determined using a NELD-PC370 concrete permeability coefficient tester (Figure 2) developed by Beijing NELD Intelligent Technology for the detection of permeable concrete during the construction of a sponge city. The tester automatically measures the permeability flow rate and time and calculates the water permeability coefficient. It is appropriate for a 100 mm cube-size specimen, which is convenient for measuring the strength after permeability measurement. Three pervious concrete specimens were tested for each mixture, and the permeability test was performed three times for consistent and reliable results. All specimens were wrapped (Figure 2) with a high-viscosity adhesive waterproof duct tape to ensure that water could not leak from the side of the specimen during the test.

(**a**) (**b**) (**c**)

Figure 2. Permeability test: (**a**) test set up; (**b**) NELD-PC370 tester; (**c**) specimens laterally wrapped.

2.4.3. Rapid Freeze–Thaw Testing

The freeze–thaw durability resistance of concrete under saturated conditions is documented by the number of freeze–thaw cycles according to GB/T50082-2009 [48]. The temperature was controlled at (−18 ± 2) °C and (22 ± 2) °C in an automatic freeze–thaw chamber. As shown in Figure 3, triplicate beam specimens with dimensions of 100 mm × 100 mm × 400 mm were tested for each mixture, and the average of three results is presented. Specimen mass loss and visual inspection were monitored every 25 cycles during the test. Each test was terminated after 300 cycles or the complete failure of the specimen. The specimens were weighed and visually inspected; the specimen's surface damage, cracks, and corner defects were carefully recorded in detail during the test.

(**a**) (**b**)

Figure 3. Specimens prior to (**a**) and during (**b**) freeze–thaw testing under saturated conditions.

2.4.4. Cantabro Abrasion Test

The Cantabro test was conducted on a Los Angeles (LA) abrasion machine without steel ball charges. Wu et al. (2011) used the Cantabro abrasion test to determine the resistance to abrasion until 300 revolutions [39]. During the test, the abrasion resistance of pervious concrete was characterized by weight loss. In this study, the weight of the specimens was determined every 100 revolutions, up to 500 revolutions. The Cantabro loss (CL) can be calculated as a percentage using the following equation:

$$CL = (W1 - W2)/(W1) \times 100 \quad (1)$$

In Equation (1), CL is the weight loss (%), W1 is the initial weight of the specimen, and W2 is the final weight of the specimen.

2.4.5. Microstructure Characterization Testing

After the compression test at 28 d, the collected samples were ground with a mortar and pestle into a fine powder and passed through an 80 µm sieve. The dried fine powder samples were weighed to 25 mg using a high-accuracy balance with a sensitivity of 0.01 mg. Fragments of size 30 mm were taken from ruptured pervious concretes after compression test at 28 d for SEM-EDS investigation. SEM-EDS investigation was performed on 30 mm fragments taken from ruptured pervious concretes after compression test at 28 d; hydration of samples was stopped using acetone. X-ray diffraction (XRD), Fourier transform infrared spectroscopy (FTIR), thermogravimetric analysis and differential thermal analysis (TGA-DTA), and scanning electron microscopy (SEM) equipped with energy dispersive spectroscopy (EDS) were employed to investigate the phase composition of the minerals and microstructure of the selected binder cement paste system in pervious concrete.

The XRD patterns were collected by X'Pert PRO diffractometer with Cu-Kα radiation (λ = 0.15419 nm) over a 2θ ranging from 5° to 70°. FTIR patterns were obtained using a Fourier transform infrared spectrometer (FTIR-650) with wave numbers ranging from 4000 to 250 cm^{-1} with a resolution of 2 cm^{-1}. TGA-DTA measurements were performed using a thermal analyzer (NETZSCH, TG 449F3 Jupiter) with a resolution of 0.01 mg, and the temperature was increased from 20 to 1000 °C at a rate of 10 °C/min. IV 9510 mercury

intrusion porosimetry (MIP) was used to characterize the pore structure and pore size distribution of hardened cement pastes in the pressure range of 0~60,000 Psi. A JEOL SX-4 scanning electron microscope (SEM) coupled with an energy dispersive spectrometer (EDS) operating at an accelerating voltage of 30 kV was employed to examine the microstructures of the selected pervious concrete and binder cement pastes.

3. Results and Discussion

3.1. Effect of Binder-to-Aggregate (B/A) Ratio on Compressive Strength and Permeability of the Reference Mixes

A series of tests were conducted to identify the impact of the B/A ratio and the incorporation of small-sized graded coarse aggregates on the compressive strength, pore structure characteristics, and permeability of pervious concrete. Five different B/A ratios (0.23, 0.25, 0.28, 0.30, and 0.32) in combination with small-sized graded coarse aggregates (4.75–9.50 mm) were used while maintaining a constant w/c ratio of 0.28 in trial mix batches. The main objective was to determine the optimum B/A ratio that could provide good mechanical properties and sufficient permeability for hardened pervious concrete without any cement paste layer agglomeration during the manufacturing and casting of the fresh mix. Figure 4a illustrates the influence of the binder-to-aggregate (B/A) ratio on the compressive strength at different curing ages. The compressive strength increased with an increase in the B/A ratio up to 0.28, indicating better aggregate-to-aggregate contact and interlocking. However, a B/A ratio higher than 0.28 led to discontinuity within the pore skeleton structure, reducing the effective porosity and permeability (similar considerations can be found in [36,49–51]). The compressive strength fluctuates within a specific range at a particular B/A ratio and does not decrease quickly.

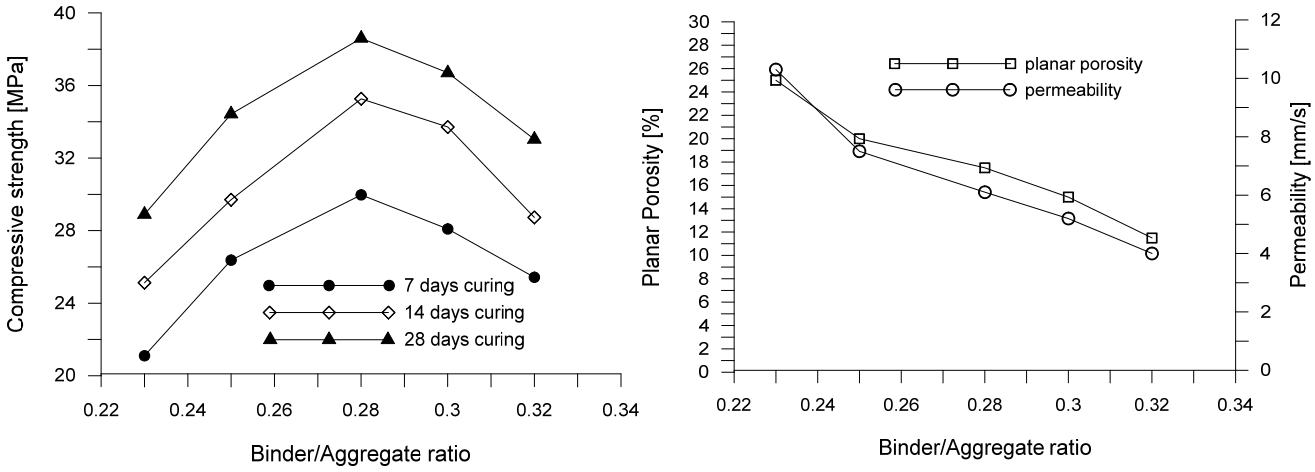

Figure 4. The effect of the binder/aggregate ratio (B/A) (**a**) on the compressive strength and (**b**) on the porosity and permeability coefficient.

In contrast, the water permeability and porosity decrease more than linearly (Figure 4b). The reduction in the compressive strength beyond the optimum B/A ratio can be attributed to the formation of distinct phases of cement filler and hydration products because of the difference in the heat of hydration, which produces discontinuous microcracks in the cement–aggregate interface (these effects are consistent with [27,35]). In this study, the optimum range of the B/A ratio is determined to be from 0.23~0.28 to obtain functional pervious concrete with good compressive strength and optimal water permeability. The permeability of pervious concrete mixes corresponding to the B/A ratio (0.23~0.32) ranges from 10.28 mm/s to 3.91 mm/s, as shown in Figure 4b. However, beyond the optimal B/A ratio of 0.28, an increase in the B/A ratio led to a 40% reduction in water permeability. This reduction indicates that more cement paste occupies the active pore voids around the

smaller aggregate particles, leading to inadequate functional properties and undermining the intended purpose of the pervious concrete.

Through trial-and-error methods, it was found that adding polycarboxylate superplasticizer (SP) to fresh concrete mixes improved the consistency and workability, resulting in stronger hardened porous concrete. Polycarboxylate superplasticizers are copolymers with long chains and high molecular mass, which wrap around cement particles to deflocculate and disperse them [28,50]. An appropriate superplasticizer dosage can ensure a homogenous and uniform porous structure throughout the cross-section of the specimen. However, a higher superplasticizer dosage can result in cement paste segregation and sedimentation with high B/A ratios, causing a reduction in the porosity and permeability of porous concrete [21,28,52].

It is crucial to control the consistency and flowability of the fresh mixture to prevent dryness from causing poor bonding between the paste and aggregate or excessive fluidity, leading to drainage into macropores [33,52]. The compressive strength and permeability of pervious concrete are significantly influenced by the coarse aggregate gradation, morphology, B/A ratio, and cement paste distribution. Therefore, selecting the appropriate coarse aggregate size and morphology, B/A ratio, and W/C ratio is primary for determining the mechanical, functional, and durability properties of pervious concrete [27,53–55]. In this study, considering the first test results, the optimum B/A ratio of 0.23 and small-sized graded coarse aggregates ranging from 4.75~9.50 mm appeared optimal to produce pervious concrete with sufficient mechanical properties and optimal permeability.

As regards the permeability/porosity, the skeleton structure and void characteristics were determined using an image analysis as in [55–57]. Figure 5 shows that the porosity and permeability are significantly correlated with the binder/aggregate (B/A) ratio. The aggregate gradation, binder/aggregate (B/A) ratio, and compaction effort substantially affect the pore size and void spatial distribution. The pore size range and interconnectivity of pores fluctuate significantly with the increase in the B/A ratio by keeping the same grade aggregate (4.75–9.50 mm) in all mixes, as the thick cementitious paste occupied the larger pore voids, thereby reducing the pore structure volume. The binary images in Figure 5 show that the pervious concrete attains a larger pore size and good connectivity of pores until the B/A ratio (0.28 in this study) corresponds to the maximum strength. Beyond this value of the B/A ratio, the pores are more refined with smaller pore sizes and are less interconnected owing to the greater cementitious paste thickness that fills the accessible macropores. The results partially confirm the studies in [55,58]. However, passing from B/A = 0.23 to B/A = 0.25, a strong reduction in permeability is observed (Figure 5). For this reason, and considering the good compressive strength obtained at B/A = 0.23, it was assumed that the combined effect of admixtures of fly ash, silica fume, and polypropylene was just for the ratio B/A = 0.23, as it will be discussed in the next section.

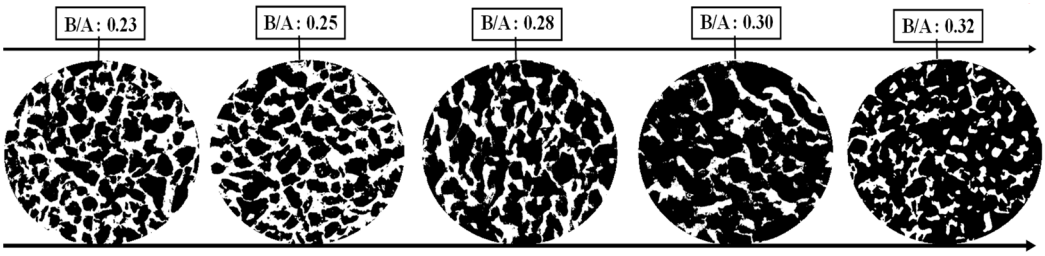

Figure 5. The skeleton pore structure of pervious concrete based on image analysis (white represents pores).

3.2. Combined Effects of Fly Ash, Silica Fume, and Polypropylene Fibers on Pervious Concrete Properties

3.2.1. Compressive Strength Development

The mix design of pervious concrete was optimized by fixing the binder-to-aggregate (B/A = 0.23) and water-to-binder (W/C = 0.28) ratios for the strength and permeability

performance. The compressive strength development of pervious concrete incorporated with fly ash and silica fume individually and combined with polypropylene fibers at various curing ages has been observed, as illustrated in Figure 6a. The substitution of 10% by weight of cement with mineral admixtures (SF and FA) in the mix design significantly enhanced the compressive strength development of porous concrete. Fly ash typically causes a delay in the pozzolanic activity. The consequence is a reduced strength at early curing. The gradual increase in pozzolanic reactivity resulted in the progressive strength development of fly ash-based concrete so that a noticeable strength is achieved at 90 days of curing compared with early curing. However, using fine sand (5%) combined with a smaller coarse aggregate and polycarboxylate superplasticizer makes the early curing strength not lower than that observed owing to the pore-filling effect and better interlock bonding of the paste–aggregate interface. This leads to the development of a dense and homogenous microstructure, which eventually enhances the compressive strength of pervious concrete [27,33,35,36,39,59,60]. Silica fume is recognized for reducing workability owing to its finer particles and larger specific surface area than cement. To compensate for the workability reduction, the literature suggests using either a chemical admixture and adjusting the water-to-cement (W/C) ratio or a suitable combination of silica fume and fly ash in the mix design to compensate for the reduction in workability [36,61]. In this study, the polycarboxylate superplasticizer maintained workability for better compaction of fresh concrete. Previous studies have also reported that adding a superplasticizer facilitates the uniform dispersion of silica fume within the mixture, thus yielding better workability and strength in silica fume-based (PC3-SF) pervious concrete [15,28,31]. The aggregate particles are wrapped and cemented together to form a skeleton-pore structure, attaining strong resistance to destructive loading at an early age. However, owing to the reduced cementitious paste content, and thus a smaller interfacial transition zone in pervious concrete, compared to conventional concrete, it is reasonable that there is no significant strength gain at longer curing ages [62].

A new formulation was considered to understand if a further enhancement of the pervious concrete strength is possible by using polypropylene fibers in the mix (PC5-PP-Rf), which is considered the reference mix for making a comparison with a binary combination of polypropylene fibers with fly ash (PC2-FAP) and silica fume (PC4-SFP). The effect of polypropylene fibers on the strength of pervious concrete is not completely clarified because of the influence of pore voids and the pore size distribution. Consequently, the reinforcing and bridging effects of fibers may be ineffective in improving the strength of reinforced pervious concrete. However, the surface vibration of the specimens may result in greater strength than rodded compacted pervious concrete, as reported in previous studies [26,32,45,63]. The low cementitious paste content in pervious concrete limits the pull strength utilization of fibers in reinforced pervious concrete (PC4-SFP). The interlocking and bridging effects between the fibers and concrete components can be improved by strengthening the cement paste with silica fume and fly ash. In addition, incorporating silica fume as a partial substitute for cement and PPFs in the mix (PC4-SFP) increased the compressive strength compared with the reference mix prepared with only fibers (PC5-PP-Rf). The results demonstrate that silica fume functions as an effective pozzolanic material to enhance the strength over time and disperse the fibers in the mixtures, leading to an improvement in the cohesiveness of the cement matrix.

Similarly, the addition of fly ash as a cement replacement and PPFs in the mix (PC2-FAP) also improved the compressive strength compared to the reference mix prepared with only fibers (PC5-PP-Rf). Finally, the mixes with a composition of fly ash and fibers or with a composition of silica fume and fibers resulted in a lower compressive strength than that obtainable by adding to the mix fly ash or silica fume without fibers. Therefore, a combination of fibers with fly ash and silica fume is justifiable if higher durability of the material or higher tensile strength is obtained or, again, if a contribution in maintaining permeability is recognized. The failure behavior of the reinforced pervious concrete was observed to be more ductile under compression tests than that of the non-reinforced

pervious concrete specimens, where specimens crumble or crush into small fragments or pieces, as shown in Figure 6b.

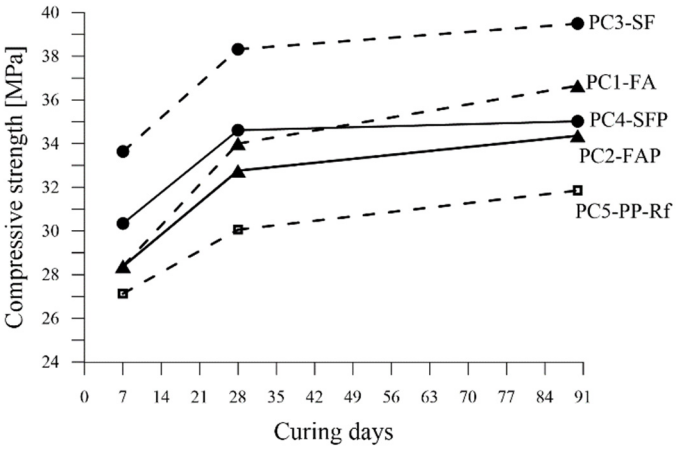

	Standard Error 7d	Standard Error 28d	Standard Error 90d
PC1-FA	0.6726	0.7664	0.8548
PC2-FP	0.6068	0.6922	0.8316
PC3-SF	0.5676	0.6938	0.882
PC4-SP	0.5674	0.6552	0.7268
PC5-PP-Rf	0.5426	0.6012	0.6866

(**a**)

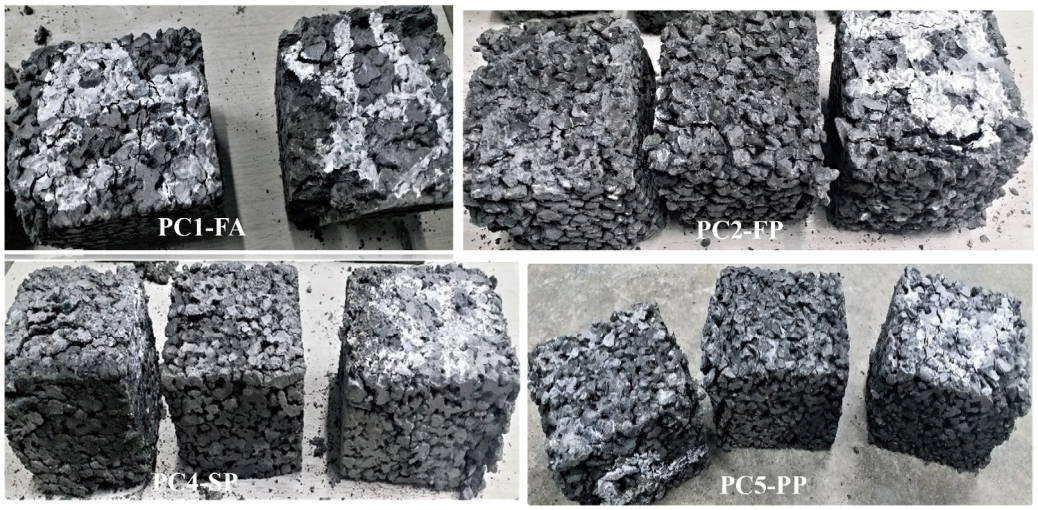

(**b**)

Figure 6. The compressive behaviour of the different mixes: (**a**) strenght vs. curing days; (**b**) failure modes.

3.2.2. Splitting Tensile and Flexural Strength

The influence of silica fume, fly ash, and polypropylene fibers on the 28-day flexural and splitting tensile strength is shown in Figure 7. The results indicate that pervious concrete mixtures containing PPFs alone (PC5-PP-Rf) or in combination with FA and SF (PC2-FAP and PC4-SFP) demonstrated higher flexural and splitting tensile strength compared to their counterparts made with FA (PC1-FA) and SF (PC3-SF). The pozzolanic reaction of SF and FA with cement hydration produced an additional C-S-H gel, which increased the fiber–matrix interface bonding by pore filling and refinement. The bridging mechanism of the fibers provided additional tensile strength to the matrix, with an increasing possibility of arresting the crack generation and propagation. Additionally, the use of smaller coarse aggregates increased the packing density of the matrix, resulting in stronger interlock bonding between the concrete components, which in turn increased the flexural and tensile strength of pervious concrete. The pervious concrete mixture (PC1-FA) attained lower flexural and splitting tensile strength due to the delayed pozzolanic reaction of fly ash at an early age.

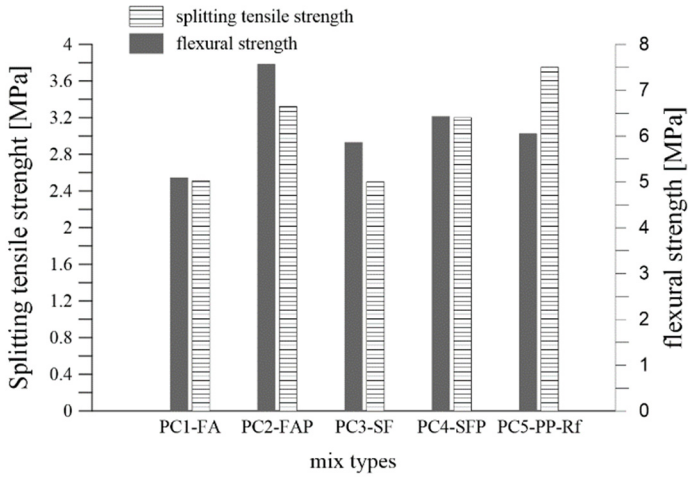

	Splitting tensile strength	Flexural strength
Mix types	Standard Error	Standard Error
PC1-FA	0.1255	0.25463
PC2-FP	0.166	0.37838
PC3-SF	0.125	0.293
PC4-SP	0.16	0.32138
PC5-PP-Rf	0.1875	0.30263

Figure 7. Splitting tensile and flexural strength. Legend: PC1-FA (mix with fly ash), PC3-SF (mix with silica fume), PC2-FAP (mix with fly ash and polypropylene fibers), PC4-SFP (mix with silica fume and polypropylene fibers), PP5-PP-Rf (reference mix with only polypropylene fibers).

The PC2-FAP and PC4-SFP mixtures showed higher flexural and split tensile strength than PC1-FA and PC3-SF. Meanwhile, PC5-PP-Rf, characterized by the presence of polypropylene fibers, exhibited an improvement lower than PC2-FAP and PC4-SFP, whose mixes contained both fibers and fly ash or fibers and silica fume. Similar observations were made regarding the flexural–compressive strength ratio. Typically, the ratio of the flexural strength to the compressive strength indicates the toughness of pervious concrete. The flexural and splitting tensile strength of pervious concrete is highly sensitive to porosity or voids in the structural skeleton, as even a slight variation in porosity can significantly impact these strengths.

3.2.3. Water Permeability

The impact of silica fume, fly ash, and polypropylene fibers on the 28-day permeability of pervious concrete is shown in Figure 8a. Mixtures made with fly ash (PC1-FA) and silica fume (PC3-SF) had lower permeability than reinforced pervious concrete mixtures. Mixtures with different porosity had distinct permeability, affected by several factors such as the aggregate size and gradation, cement paste thickness, binder/aggregate ratio, W/C ratio, fine aggregate, and compaction effort. As shown in Figure 8a, the permeability of the mixtures containing PPFs along with silica fume (PC4-SFP) and fly ash (PC2-FAP) was lower compared to the reference mixture made with only PPFs (PC5-PP-Rf). The inclusion of silica fume and fly ash occupied the pore voids in pervious concrete via pore filling and densification of the cement matrix by the pozzolanic reaction with cement hydration products, thereby reducing the connected porosity and ultimately reducing the permeability. On the other hand, in comparison with a mixture produced with silica fume (PC3-SF) and fly ash (PC1-FA), there was an increase in permeability when fly ash and silica fume were used in combination with polypropylene fibers (PC4-SFP and PC2-FAP). The increase in permeability with the addition of fibers may be related to the formation of interconnected channels between the fiber and cement matrix interface due to relatively inferior adhesion bonding, which increases the connected porosity of reinforced pervious concrete. The increase in connected porosity permits more water to percolate through the interconnected pores, which is responsible for increased permeability.

The studies in the literature are contrasting. If, on the one hand, some of them have reported an increase in permeability with fiber addition, e.g., [42], some others have found a decrease in porosity and permeability with fiber incorporation, e.g., [32]. In contrast, Singh et al. [40] found no significant effect of fibers on the porosity and permeability of reinforced pervious concrete.

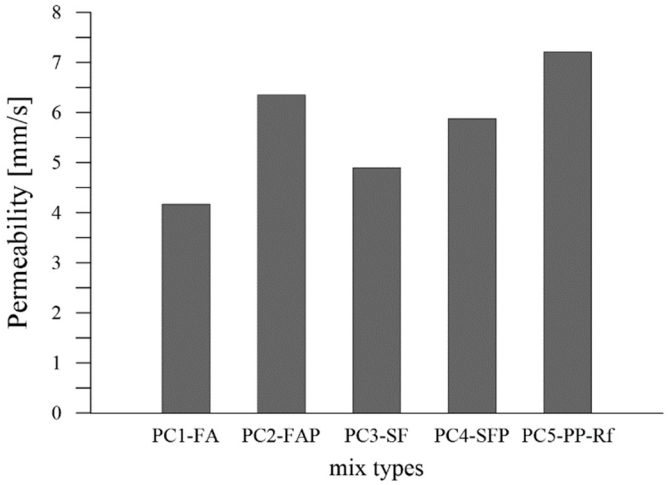

Mix type	Standard error
PC1-FA	0.11
PC2-FP	0.34
PC3-SF	0.31
PC4-SP	0.32
PC5-PP-Rf	0.36

(**a**)

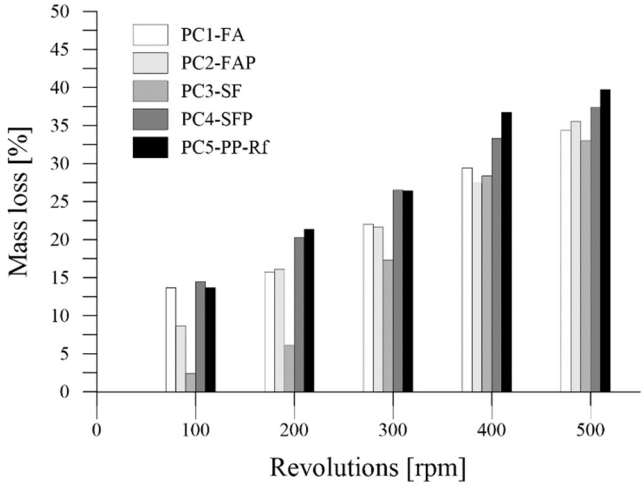

(**b**)

Figure 8. Permeability (**a**) and Cantabro mass loss (**b**) after 28 d of curing.

3.3. Durability of Pervious Concrete

The durability of the pervious concrete was assessed based on the raveling and freeze–thaw resistance. The raveling resistance was measured using the Cantabro mass loss test, and the freeze–thaw resistance was determined at (-18 ± 2) °C and (22 ± 2) °C in a freeze–thaw chamber to determine the damage mechanism.

3.3.1. Raveling Resistance

The influence of silica fume, fly ash, and polypropylene fibers on the 28-day raveling resistance is shown in Figure 8b. Mass loss manifests the abrasion quality during the (LA) abrasion test. The incorporation of cementitious materials (such as SF and FA) along with fiber reinforcement provides bridging mechanisms between the components of pervious concrete. Figure 8b shows that the mass loss associated with the deterioration of the specimens increased with an increase in the number of cycles. After 500 cycles, all mixtures exhibited a failure pattern, where coarse aggregates detached from the surface and corner edges, resulting in progressive damage. The PC3-SF mixture exhibited the lowest mass loss (<22%) due to its dense microstructure and improved interlocking strength resulting from the physical filling effect and the pozzolanic reaction of silica fume. The fly ash-based mixture, PC1-FA, showed a more significant mass loss during the test than PC3-SF because of the later strength gain of PC1-FA, owing to the delayed pozzolanic reaction. The use

of PPFs with fly ash (PC2-FAP) and silica fume (PC4-SFP) resulted in a slightly higher final mass loss than the mixture with fly ash (PC1-FA) and silica fume (PC3-SF). This increase in mass loss could be attributed to the higher porosity and permeability of the mixes containing PPFs in this study. For the same reason, the inclusion of PPFs without other admixtures decreased the overall degradation resistance.

3.3.2. Freeze–Thaw Resistance

The impact of silica fume, fly ash, and polypropylene fibers on the 28-day freeze–thaw resistance of pervious concrete is shown in Figure 9. The freeze–thaw resistance can be divided into three stages. During stage I, no noteworthy variation in mass loss was observed (until 100 cycles). In stage I of freeze–thaw cycling, the degree of saturation (DOS) was low, and insignificant deterioration occurred, except for PC2-FAP with a higher DOS. In stage II, the mass loss variation was more evident owing to the raveling or disintegration of aggregates, debonding, and cement paste spalling. The mass loss of the fly ash-based mixture (PC1-FA) and fiber-reinforced fly ash mixture (PC2-FAP) grew much faster and was accelerated by the substantial uptake of water during consecutive freeze–thaw cycles.

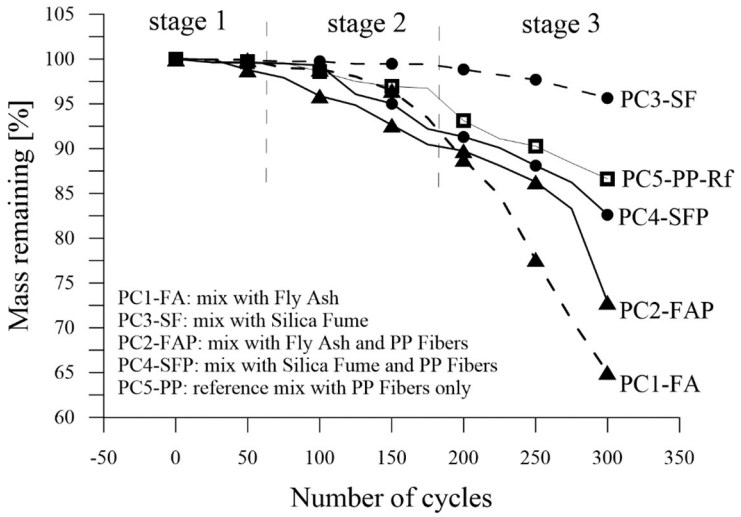

Figure 9. Freeze-thaw durability performance based on mass loss criteria.

During stage II, the frost-heaving stress (FHS) builds up with a critical degree of saturation, leading to serious micro-damage development with a progressive increase in freeze–thaw cycling. The FHS depends on the air voids and the degree of saturation of the specimens; therefore, mixtures with more air voids and full saturation exhibited more mass loss and a higher degree of damage evolution (this condition has also been observed in [64]). In stage III, the variation in the mass loss was more abrupt and sharp, indicating serious micro- and macro-damage evolution, with obvious surface cracks developing in the specimens that partially passed through the cement paste, and the aggregate interface further aggravated the debonding of the aggregate with increasing freeze–thaw cycling. A silica fume-based (PC3-SF) mixture with a dense microstructure increased the resistance to frost damage during all three stages of freeze–thaw cycling. The incorporation of fibers in pervious concrete provides a reinforcing effect to bridge the crack propagation and strengthen the bond among concrete components, thus efficiently enhancing the freeze–thaw performance of reinforced (PC5-PP-Rf) pervious concrete. The effectiveness of PPFs in enhancing the freeze–thaw performance of silica fume (PC4-SFP) and fly ash-based (PC2-FAP) reinforced mixes were found to be highly distinct, which was attributed to their unique pore structure characteristics. In stage III, the deterioration rate was drastic because the bridging mechanisms of the fiber were not capable of avoiding the cracks and resisting the expansive stresses built up during the continuous freeze–thaw cycling; thus, a slight improvement in the freeze–thaw performance was achieved.

3.4. Hydration Product Analysis of the Cement Past Containing Fly Ash and Silica Fume

3.4.1. TGA-DTA Measurement

The TGA-DTA curves of cement paste containing fly ash (FPC1) and silica fume (SPC2) are illustrated in Figure 10. Three different major endothermic peaks occurred in the temperature ranges of 100–150 °C, 400–500 °C, and 700–800 °C. The first endothermic peaks found at 100–150 °C were primarily due to the dehydroxylation of the calcium silicate hydrate (C-S-H) phase. The second endothermic peak identified at 400–500 °C is attributed to the dehydration and decomposition of portlandite $Ca(OH)_2$ (this is consistent with [65,66]). The addition of fly ash substantially influences the DTA profile, causing a reduction in the endothermic peaks at higher temperatures. Calcium carbonate decomposition occurs at 700~800 °C. The analysis of TG and DTG results indicates that the addition of fly ash or silica fume enhances the formation of hydration products through a pozzolanic reaction.

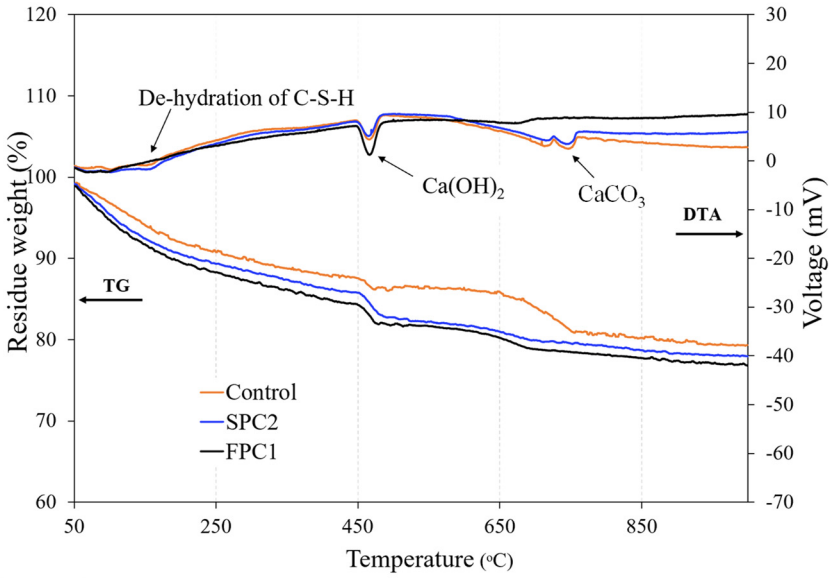

Figure 10. TGA-DTA profiles of control and binder cement pastes after 28 days.

3.4.2. XRD Spectra

The XRD diffractograms of the standard and blended cement pastes at 28 days are shown in Figure 11a. The relative peak intensity of $Ca(OH)_2$ in the blended paste (SPC2) was lower than that of the reference paste without silica fume. However, stronger $Ca(OH)_2$ peaks were observed for the fly ash-blended paste (FPC1) because of its slower pozzolanic reactivity. It is reported that the pozzolanic reactivity of fly ash is slower than cement hydration, and the extent of fly ash reaction for blended paste with a water/binder ratio (W/C) equal to 0.5 and an FA content of 25% is approximately 10% to 14% at the age of 28 days. According to Hanehara et al. [67], the extent of fly ash reactivity increased to approximately 25% at the age of 1 year for blended cement paste produced with a W/C ratio of 0.5 and an FA content of 40%. The $CaCO_3$ peaks observed in all pastes could be attributed to natural carbonation. The precipitation of $Ca(OH)_2$ and C-S-H on the etched surface of fly ash particles, with an increase in the pozzolanic reaction, reinforces the contact bonding between fly ash and cement as well as fly ash particles. This would ultimately make the microstructure denser and more homogeneous and result in a remarkable long-term strength gain.

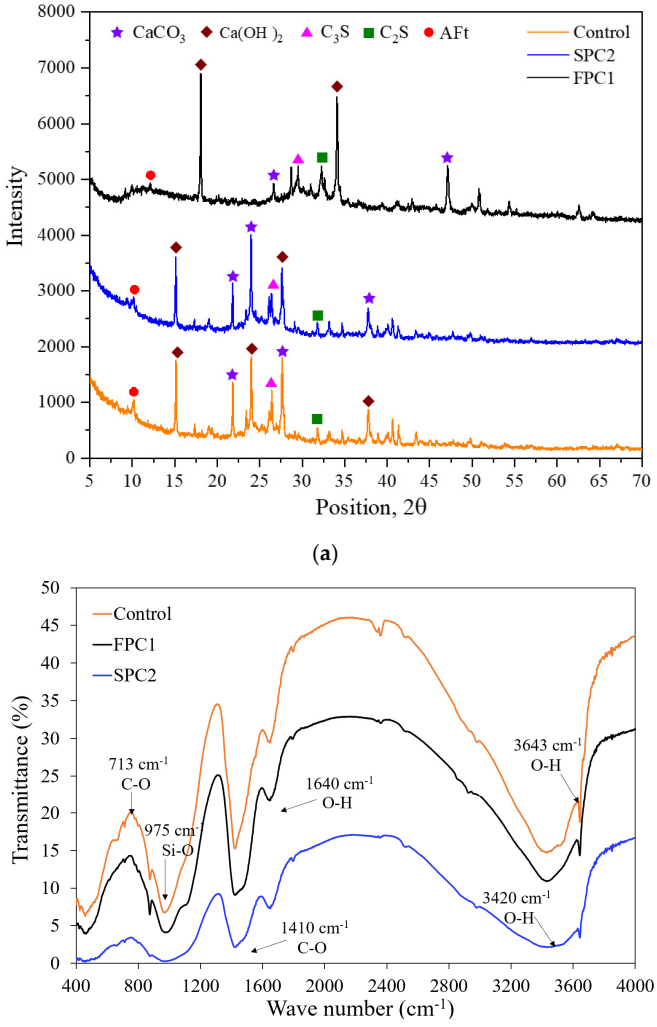

Figure 11. XRD spectrum (**a**) and FTIR spectra (**b**) of control and binder cement paste at 28 days of standard curing.

3.4.3. FTIR Spectra Analysis

FTIR measurements were performed to demonstrate the mineral variations caused by fly ash in FPC1 and silica fume in the SPC2 mix, as shown in Figure 11b. The absorption peaks at 3420 cm^{-1} are attributed to the vibrational bending of O-H groups in water, and the bending at 1640 cm^{-1} is associated with the O-H groups. The other O-H band at 3643 cm^{-1} originated from the O-H bond in $Ca(OH)_2$, which reduced the pattern of the modified samples, indicating that $Ca(OH)_2$ was consumed by the SCMs in the pastes. The Si-O stretching vibration band at 975 cm^{-1} represents the C-S-H gel with systematically changing frequency and intensity with the CaO/SiO_2 ratio in C-S-H.

3.5. Microstructure Characteristics

3.5.1. Pore Structure

Mercury intrusion porosimetry (MIP) is a widely used technique for assessing the porosity and distribution of pore sizes in cement-based materials. Figure 12 shows the influence of silica fume and fly ash on the pore structure evolution and pore size distribution of the blended cement pastes after 28 days of curing. The pore size distribution of each mixture ranged from 0 to 10 µm. The specific pore volume exhibited a slight variation with an increase in pore diameter (>100 nm); however, a significant increase in pore volume was observed in the range of pore diameters less than 100 nm, as shown in Figure 12a. The

higher cumulative pore volume with fly ash is due to the lower pozzolanic reaction; as the reaction activates, the total pore volume and pore size would reduce. The differential curve in Figure 12b shows an unimodal pore size distribution, with the largest pore volume located at 26.30 nm for all mixes. The probable pore diameter corresponding to the peak of each differential curve reflects the refinement of pores and the pore size distribution shifts toward smaller pore size ranges. According to Zeng et al. (2012) [68], the measured pore size distribution can be classified into four size ranges: gel micropores (<10 nm), mesopores (10–50 nm), middle capillary pores (50–100 nm), and large capillary pores (>100 nm). The volume ratio of mesopores was the highest, followed by middle capillary pores for all mixes. The inclusion of silica fume and fly ash in blended pastes densifies the microstructure by pore filling and the pozzolanic reaction, which reduces the harmful macrocapillary pores (>50 nm) that are detrimental to the strength and increases the mesopores, which are less harmful to the strength of concrete.

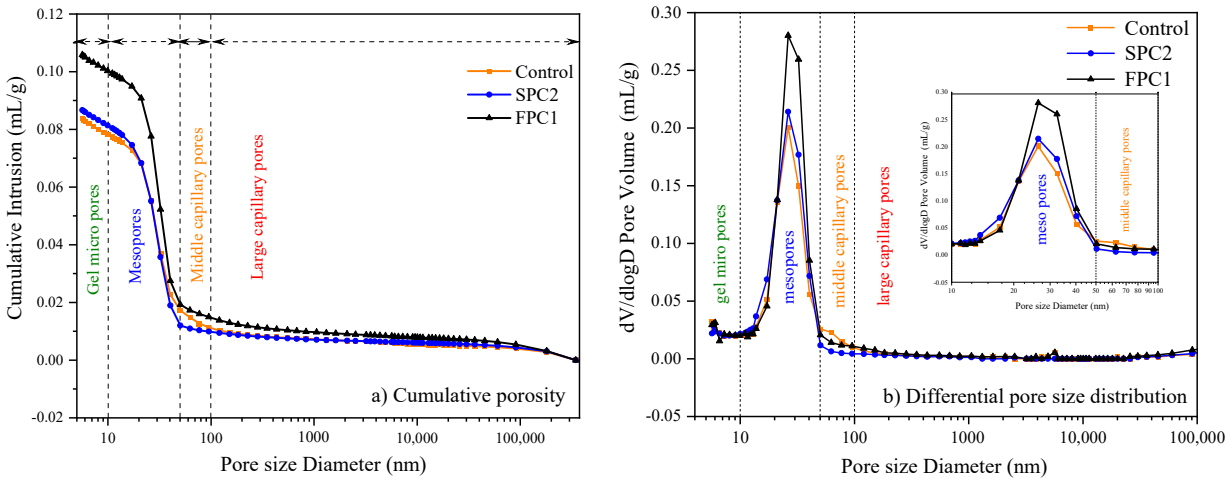

Figure 12. The porosity (**a**) and pore size distribution (**b**) of control and blended cement pastes at 28 days of standard curing.

3.5.2. Microstructure Morphology of Porous Concrete

SEM micrographs of fly ash, silica fume, and fiber-based pervious concrete after the compressive strength test are shown in Figures 13–15. A few partially reacted and broken fly ash particles with etched surfaces and hydrated rim encapsulation can be observed in Figure 13. The precipitation of $Ca(OH)_2$ and C-S-H on the etched surface of fly ash particles with an increase in the pozzolanic reaction reinforces the contact bonding between fly ash and cement, as well as fly ash particles, making the microstructure denser and more homogeneous and resulting in a remarkable long-term strength gain. The cracks detected in the SEM micrographs were assumed to be due to the compression strength test performed before the SEM investigation. In general, the elemental composition determined by EDS analysis indicates that Ca, O, Si, and Ai are the major elements comprising the C-S-H and C-A-S-H gels in the cementitious composite.

In PC5-PP-Rf, a few hydration particles and striations are visible on the fiber surface (Figure 15). In contrast, the PC2-FAP and PC4-SFP mixtures exhibited dense hydration products on the polypropylene fibers, leading to improved adhesion bonding between the interface matrix and the fibers. This enhanced the flexural strength of the reinforced porous concrete by increasing the bridging and pull-out resistance. The presence of fly ash and silica fume particles refines the pore enlargement caused by PPFs in the cement interface matrix through a micro-filling ability and pozzolanic reactions, which improves the mechanical properties of reinforced porous concrete. Proper amounts of PPFs combined with fly ash and silica fume ensured a uniform distribution throughout the matrix, enhancing the stress transformation between the interface matrix and fibers in the reinforced porous concrete.

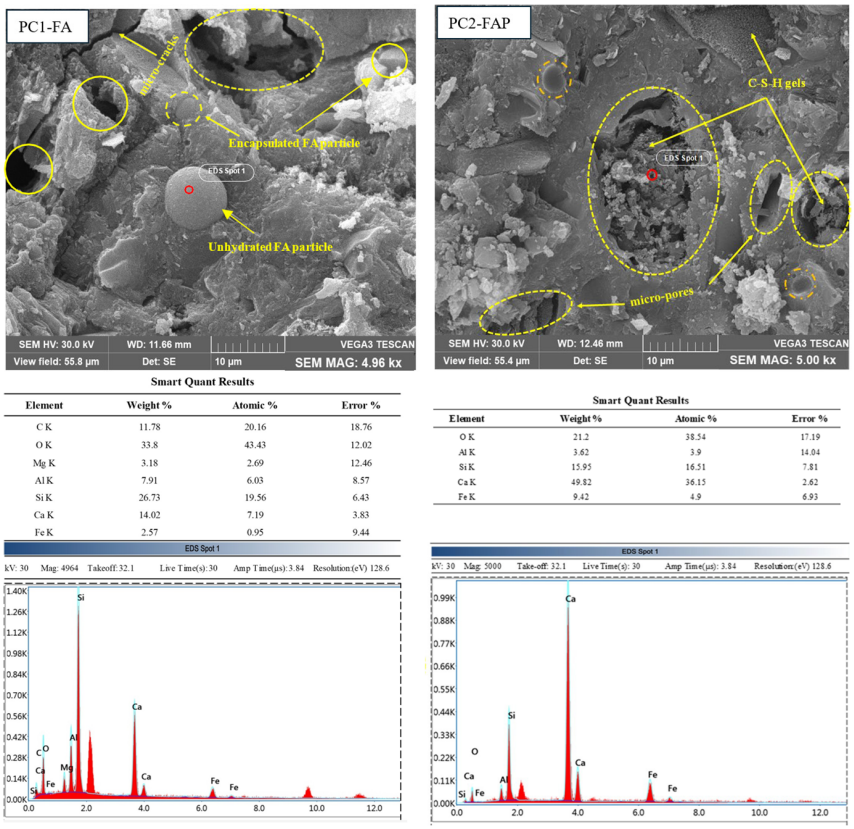

Figure 13. SEM and EDS micrographs of porous concrete after 28 days of standard curing: PC1-FA and PC2-FAP.

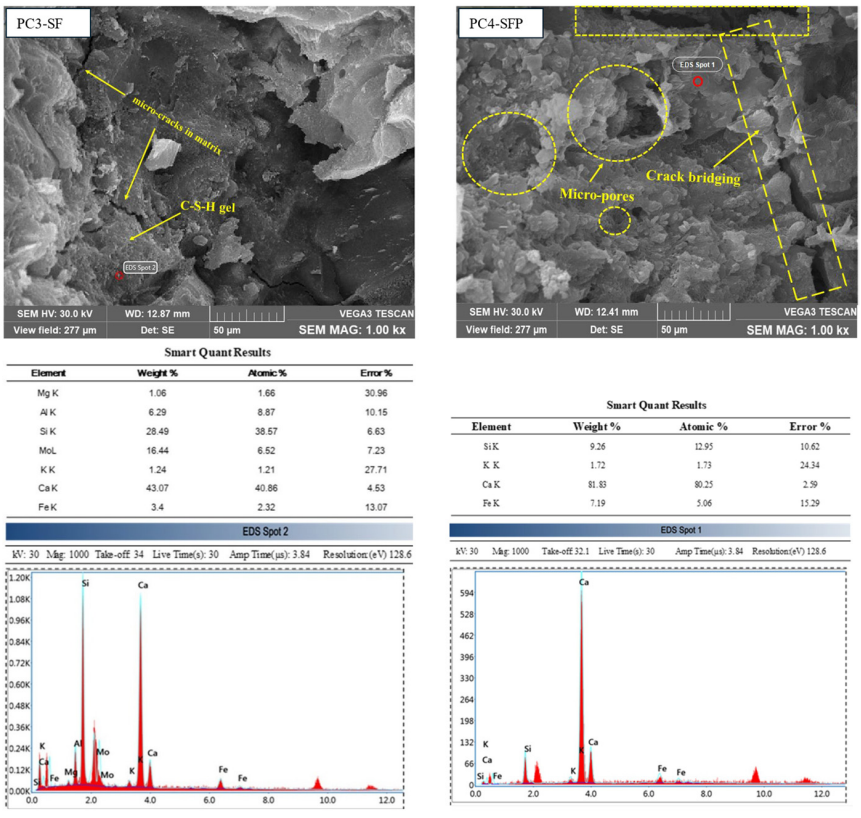

Figure 14. SEM and EDS micrographs of porous concrete after 28 days of standard curing: PC3-SF and PC4-SFP.

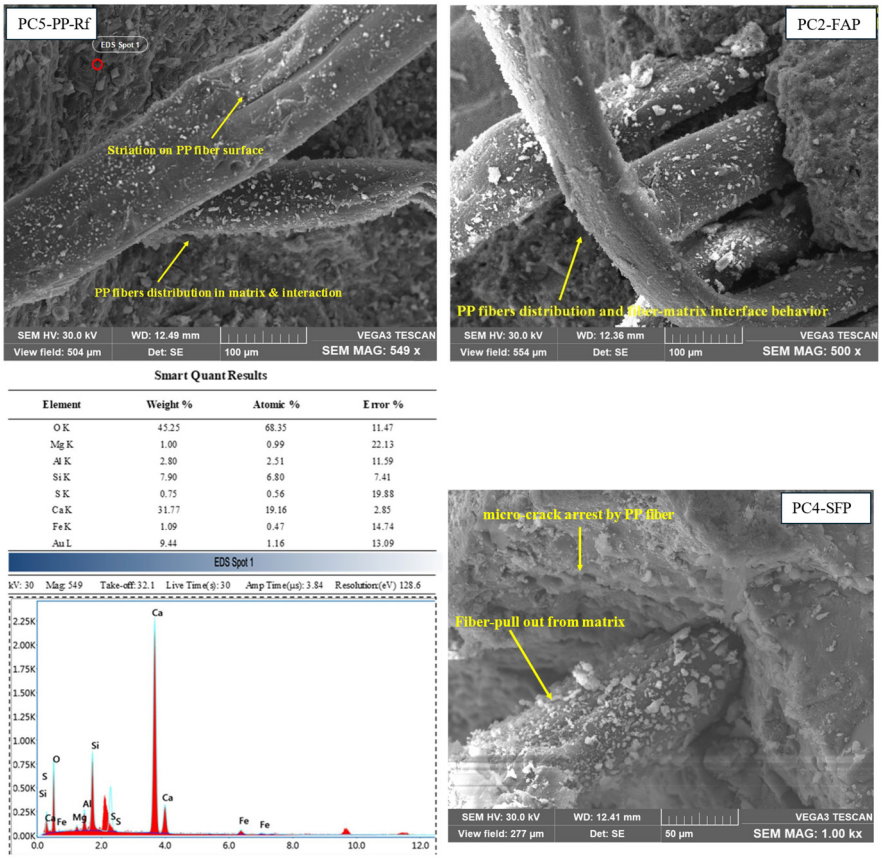

Figure 15. SEM and EDS micrographs of porous concrete after 28 days of standard curing: PC5-PP-Rf, PC2-FAP, and PC4SFP.

4. Conclusions

The following conclusions were derived by examining the impact of the B/A ratio, 5% fine sand, 10% fly ash or silica fume, and a binary combination of 10% fly ash or silica fume with 0.2% PPFs on the mechanical and durability characteristics of pervious concrete.

1. The binder-to-aggregate (B/A) ratio and compaction determine the strength and pore structure characteristics of the pervious concrete. The compressive strength increased with the B/A ratio up to an optimum limit of 0.28 and decreased beyond this limit. On the other hand, the increase in the B/A ratio always causes a reduction in porosity and permeability. Therefore, the choice of an appropriate B/A ratio requires the study of the variation in the skeleton pore structure. For the type of mix analyzed, the value of the B/A ratio being equal to 0.23 guarantees a good compromise that provides good compressive strength and optimal permeability.
2. Pervious concrete produced with fly ash or silica fume achieved the highest compressive strength (>35 MPa) at 28 days but had inferior flexural and tensile strengths compared to fiber-reinforced pervious concrete. The permeability was reduced by 10% fly ash or silica fume with 5% fine sand in pervious concrete; however, the binary combination of either fly ash or silica fume with polypropylene fibers enhanced the pore connectivity, thus yielding higher strength indices with adequate permeability greater than 5 mm/s.
3. Silica fume with fiber-reinforced pervious concrete exhibited the lowest mass loss based on abrasion and F-T durability performance criteria. Fiber-reinforced pervious concrete showed a similar mass loss to the silica fume fiber-reinforced based mix but improved the overall degradation resistance by reinforcing and bridging the aggregate and cementitious matrix together. Fly ash-based mixtures demonstrated

more significant mass loss due to the substantial uptake of water during consecutive F-T cycles.

4. Microstructural analysis showed that pervious concrete produced with an appropriate amount of PPFs and fly ash or silica fume led to a uniform distribution of fibers in the matrix, thus improving the stress transformation between the interface matrix and the fibers through bridging effects in the reinforced pervious concrete. The inclusion of fly ash or silica fume reduced the harmful capillary pores and refined the pore enlargement caused by PPFs in the cement interface matrix through micro-filling and a pozzolanic reaction, leading to improved mechanical properties and durability characteristics of pervious concrete.
5. The durability of reinforced pervious concrete, particularly in terms of its clogging resistance, is crucial for maintaining its long-term permeability. This aspect has not been investigated in this study; therefore, the conclusions and the results should be coupled with the clogging resistance characteristics to be obtained by further experimental studies.
6. The characteristics (mechanical and physical) of pervious concrete here proposed and investigated comply with the requirements of the specific standard codes for pervious concrete (e.g., the American ACI SPEC-522.1-13 [69] or the Chinese CJJ/T 135-2009 [70] and JC/T 2558-2020 [71]). Therefore, each mix is suitable for practical applications that are consistent with the objectives of the users.

Author Contributions: Conceptualization, X.G., L.C., H.B. and M.R.; methodology, X.G., H.B. and M.R.; software, H.B., L.C. and A.K.; validation, X.G., L.C., H.B., M.R. and AK.; formal analysis, H.B.; investigation, H.B. and M.R.; resources, X.G.; data curation, H.B.; writing—original draft preparation, H.B.; writing—review and editing, X.G., L.C. and M.R.; visualization, H.B., L.C. and A.K.; supervision, X.G. and L.C.; project administration, X.G. and M.R.; funding acquisition, X.G. All authors have read and agreed to the published version of the manuscript.

Funding: This research was funded by the Provincial Applied Technology Research and Development Major Project, grant number GA20C010 and the Natural Science Foundation of Heilongjiang Province of China, grant number LH2021E113.

Data Availability Statement: The original contributions presented in the study are included in the article; further inquiries can be directed to the corresponding author.

Acknowledgments: The authors would like to acknowledge the administrative and technical support provided by the School of Civil Engineering, Harbin Institute of Technology, China, particularly those research fellows in the Civil Engineering Materials Research Group, during the preparation and experimental testing.

Conflicts of Interest: The authors declare no conflicts of interest. The funders had no role in the design of the study; in the collection, analyses, or interpretation of data; in the writing of the manuscript; or in the decision to publish the results.

Abbreviations

B/A	Binder-to-aggregate ratio
A/B	Aggregate-to-binder ratio
W/C	Water-to-cement ratio
SP	Superplasticizer
PPFs	Polypropylene fibers
FHS	Frost-heaving stress
FA	Fly ash
SF	Silica fume
XRD	X-ray diffraction
FTIR	Fourier transform infrared spectroscopy
SEM	Scanning electron microscopy
EDS	Energy dispersive spectroscopy

XRF.	X-ray fluorescence spectrometry
TGA	Thermogravimetric analysis
DTA	Differential thermal analysis
SEM-EDS	Scanning electron microscopy equipped with energy dispersive spectroscopy
MIP	Mercury intrusion porosimetry

References

1. Sahdeo, S.K.; Ransinchung, G.D.; Rahul, K.L.; Debbarma, S. Effect of Mix Proportion on the Structural and Functional Properties of Pervious Concrete Paving Mixtures. *Constr. Build. Mater.* **2020**, *255*, 119260. [CrossRef]
2. Khankhaje, E.; Salim, M.R.; Mirza, J.; Salmiati; Hussin, M.W.; Khan, R.; Rafieizonooz, M. Properties of Quiet Pervious Concrete Containing Oil Palm Kernel Shell and Cockleshell. *Appl. Acoust.* **2017**, *122*, 113–120. [CrossRef]
3. Chu, L.; Fwa, T.F.; Tan, K.H. Laboratory Evaluation of Sound Absorption Characteristics of Pervious Concrete Pavement Materials. *Transp. Res. Rec. J. Transp. Res. Board* **2017**, *2629*, 91–103. [CrossRef]
4. Li, H.; Harvey, J.; Ge, Z. Experimental Investigation on Evaporation Rate for Enhancing Evaporative Cooling Effect of Permeable Pavement Materials. *Constr. Build. Mater.* **2014**, *65*, 367–375. [CrossRef]
5. Guan, X.; Wang, J.; Xiao, F. Sponge City Strategy and Application of Pavement Materials in Sponge City. *J. Clean. Prod.* **2021**, *303*, 127022. [CrossRef]
6. Li, H.; Ding, L.; Ren, M.; Li, C.; Wang, H. Sponge City Construction in China: A Survey of the Challenges and Opportunities. *Water* **2017**, *9*, 594. [CrossRef]
7. Wang, C.; Hou, J.; Miller, D.; Brown, I.; Jiang, Y. Flood Risk Management in Sponge Cities: The Role of Integrated Simulation and 3D Visualization. *Int. J. Disaster Risk Reduct.* **2019**, *39*, 101139. [CrossRef]
8. Ding, L.; Ren, X.; Gu, R.; Che, Y. Implementation of the "Sponge City" Development Plan in China: An Evaluation of Public Willingness to Pay for the Life-Cycle Maintenance of Its Facilities. *Cities* **2019**, *93*, 13–30. [CrossRef]
9. Hou, X.; Guo, H.; Wang, F.; Li, M.; Xue, X.; Liu, X.; Zeng, S. Is the Sponge City Construction Sufficiently Adaptable for the Future Stormwater Management under Climate Change? *J. Hydrol.* **2020**, *588*, 125055. [CrossRef]
10. Nguyen, T.T.; Ngo, H.H.; Guo, W.; Wang, X.C. A New Model Framework for Sponge City Implementation: Emerging Challenges and Future Developments. *J. Environ. Manage.* **2020**, *253*, 109689. [CrossRef]
11. Li, Q.; Wang, F.; Yu, Y.; Huang, Z.; Li, M.; Guan, Y. Comprehensive Performance Evaluation of LID Practices for the Sponge City Construction: A Case Study in Guangxi, China. *J. Environ. Manage.* **2019**, *231*, 10–20. [CrossRef] [PubMed]
12. López-Carrasquillo, V.; Hwang, S. Comparative Assessment of Pervious Concrete Mixtures Containing Fly Ash and Nanomaterials for Compressive Strength, Physical Durability, Permeability, Water Quality Performance and Production Cost. *Constr. Build. Mater.* **2017**, *139*, 148–158. [CrossRef]
13. Grubeša, I.N.; Barišić, I.; Ducman, V.; Korat, L. Draining Capability of Single-Sized Pervious Concrete. *Constr. Build. Mater.* **2018**, *169*, 252–260. [CrossRef]
14. Zhang, G.; Wang, S.; Wang, B.; Zhao, Y.; Kang, M.; Wang, P. Properties of Pervious Concrete with Steel Slag as Aggregates and Different Mineral Admixtures as Binders. *Constr. Build. Mater.* **2020**, *257*, 119543. [CrossRef]
15. Adil, G.; Kevern, J.T.; Mann, D. Influence of Silica Fume on Mechanical and Durability of Pervious Concrete. *Constr. Build. Mater.* **2020**, *247*, 118453. [CrossRef]
16. Giustozzi, F. Polymer-Modified Pervious Concrete for Durable and Sustainable Transportation Infrastructures. *Constr. Build. Mater.* **2016**, *111*, 502–512. [CrossRef]
17. Wu, H.; Liu, Z.; Sun, B.; Yin, J. Experimental Investigation on Freeze–Thaw Durability of Portland Cement Pervious Concrete (PCPC). *Constr. Build. Mater.* **2016**, *117*, 63–71. [CrossRef]
18. Yang, Z. Freezing-and-Thawing Durability of Pervious Concrete under Simulated Field Conditions. *Mater. J.* **2011**, *108*, 187–195.
19. Huang, B.; Wu, H.; Shu, X.; Burdette, E.G. Laboratory Evaluation of Permeability and Strength of Polymer-Modified Pervious Concrete. *Constr. Build. Mater.* **2010**, *24*, 818–823. [CrossRef]
20. Shu, X.; Huang, B.; Wu, H.; Dong, Q.; Burdette, E.G. Performance Comparison of Laboratory and Field Produced Pervious Concrete Mixtures. *Constr. Build. Mater.* **2011**, *25*, 3187–3192. [CrossRef]
21. Bilal, H.; Chen, T.; Ren, M.; Gao, X.; Su, A. Influence of Silica Fume, Metakaolin & SBR Latex on Strength and Durability Performance of Pervious Concrete. *Constr. Build. Mater.* **2021**, *275*, 122124. [CrossRef]
22. Nguyen, D.H.; Boutouil, M.; Sebaibi, N.; Baraud, F.; Leleyter, L. Durability of Pervious Concrete Using Crushed Seashells. *Constr. Build. Mater.* **2017**, *135*, 137–150. [CrossRef]
23. Ibrahim, H.A.; Abdul Razak, H.; Abutaha, F. Strength and Abrasion Resistance of Palm Oil Clinker Pervious Concrete under Different Curing Method. *Constr. Build. Mater.* **2017**, *147*, 576–587. [CrossRef]
24. Gesoğlu, M.; Güneyisi, E.; Khoshnaw, G.; İpek, S. Abrasion and Freezing–Thawing Resistance of Pervious Concretes Containing Waste Rubbers. *Constr. Build. Mater.* **2014**, *73*, 19–24. [CrossRef]
25. Gaedicke, C.; Marines, A.; Miankodila, F. Assessing the Abrasion Resistance of Cores in Virgin and Recycled Aggregate Pervious Concrete. *Constr. Build. Mater.* **2014**, *68*, 701–708. [CrossRef]

26. Toghroli, A.; Mehrabi, P.; Shariati, M.; Trung, N.T.; Jahandari, S.; Rasekh, H. Evaluating the Use of Recycled Concrete Aggregate and Pozzolanic Additives in Fiber-Reinforced Pervious Concrete with Industrial and Recycled Fibers. *Constr. Build. Mater.* **2020**, *252*, 118997. [CrossRef]
27. Dai, Z.; Li, H.; Zhao, W.; Wang, X.; Wang, H.; Zhou, H.; Yang, B. Multi-Modified Effects of Varying Admixtures on the Mechanical Properties of Pervious Concrete Based on Optimum Design of Gradation and Cement-Aggregate Ratio. *Constr. Build. Mater.* **2020**, *233*, 117178. [CrossRef]
28. Lian, C.; Zhuge, Y. Optimum Mix Design of Enhanced Permeable Concrete—An Experimental Investigation. *Constr. Build. Mater.* **2010**, *24*, 2664–2671. [CrossRef]
29. Zhong, R.; Wille, K. Compression Response of Normal and High Strength Pervious Concrete. *Constr. Build. Mater.* **2016**, *109*, 177–187. [CrossRef]
30. Lang, L.; Duan, H.; Chen, B. Properties of Pervious Concrete Made from Steel Slag and Magnesium Phosphate Cement. *Constr. Build. Mater.* **2019**, *209*, 95–104. [CrossRef]
31. Yang, J.; Jiang, G. Experimental Study on Properties of Pervious Concrete Pavement Materials. *Cem. Concr. Res.* **2003**, *33*, 381–386. [CrossRef]
32. Kevern, J.T.; Biddle, D.; Cao, Q. Effects of Macrosynthetic Fibers on Pervious Concrete Properties. *J. Mater. Civ. Eng.* **2015**, *27*, 06014031. [CrossRef]
33. Huang, J.; Luo, Z.; Khan, M.B.E. Impact of Aggregate Type and Size and Mineral Admixtures on the Properties of Pervious Concrete: An Experimental Investigation. *Constr. Build. Mater.* **2020**, *265*, 120759. [CrossRef]
34. Saboo, N.; Shivhare, S.; Kori, K.K.; Chandrappa, A.K. Effect of Fly Ash and Metakaolin on Pervious Concrete Properties. *Constr. Build. Mater.* **2019**, *223*, 322–328. [CrossRef]
35. Wang, H.; Li, H.; Liang, X.; Zhou, H.; Xie, N.; Dai, Z. Investigation on the Mechanical Properties and Environmental Impacts of Pervious Concrete Containing Fly Ash Based on the Cement-Aggregate Ratio. *Constr. Build. Mater.* **2019**, *202*, 387–395. [CrossRef]
36. Nazeer, M.; Kapoor, K.; Singh, S.P. Strength, Durability and Microstructural Investigations on Pervious Concrete Made with Fly Ash and Silica Fume as Supplementary Cementitious Materials. *J. Build. Eng.* **2023**, *69*, 106275. [CrossRef]
37. Kevern, J.; Wang, K.; Suleiman, M.T.; Schaefer, V.R. Mix Design Development for Pervious Concrete in Cold Weather Cli-Mates. In Proceedings of the 2005 Mid-Continent Transportation Research Symposium, Ames, IA, USA, 18–19 August 2005; Iowa State University: Ames, IA, USA, 2005. Available online: https://rosap.ntl.bts.gov/view/dot/38663/dot_38663_ds1.pdf (accessed on 1 October 2024).
38. Kevern, J.T.; Schaefer, V.R.; Wang, K.; Suleiman, M.T. Pervious Concrete Mixture Proportions for Improved Freeze-Thaw Durability. *J. ASTM Int.* **2008**, *5*, 1–12. [CrossRef]
39. Wu, H.; Huang, B.; Shu, X.; Dong, Q. Laboratory Evaluation of Abrasion Resistance of Portland Cement Pervious Concrete. *J. Mater. Civ. Eng.* **2011**, *23*, 697–702. [CrossRef]
40. Bright Singh, S.; Murugan, M. Effect of Aggregate Size on Properties of Polypropylene and Glass Fibre-Reinforced Pervious Concrete. *Int. J. Pavement Eng.* **2022**, *23*, 2034–2048. [CrossRef]
41. Juradin, S.; Netinger-Grubeša, I.; Mrakovčić, S.; Jozić, D. Impact of Fibre Incorporation and Compaction Method on Properties of Pervious Concrete. *Mater. Constr.* **2021**, *71*, e245. [CrossRef]
42. Furkan Ozel, B.; Sakallı, Ş.; Şahin, Y. The Effects of Aggregate and Fiber Characteristics on the Properties of Pervious Concrete. *Constr. Build. Mater.* **2022**, *356*, 129294. [CrossRef]
43. Akand, L.; Yang, M.; Wang, X. Effectiveness of Chemical Treatment on Polypropylene Fibers as Reinforcement in Pervious Concrete. *Constr. Build. Mater.* **2018**, *163*, 32–39. [CrossRef]
44. Wu, J.; Hu, L.; Hu, C.; Wang, Y.; Zhou, J.; Li, X. Impact of Polypropylene Fiber on the Mechanical and Physical Properties of Pervious Concrete: An Experimental Investigation. *Buildings* **2023**, *13*, 1966. [CrossRef]
45. Qin, L.; Gao, X.; Chen, T. Influence of Mineral Admixtures on Carbonation Curing of Cement Paste. *Constr. Build. Mater.* **2019**, *212*, 653–662. [CrossRef]
46. *GT/B 50081–2002*; Standard for Test Method of Mechanical Properties in Ordinary Concrete. Ministry of Housing and Urban-Rural Development of China (MOHURD): Beijing, China, 2002.
47. *GT/B 50082-2009*; Revised Standard for Test Methods of Long-Term Performance and Durability of Ordinary Concrete. Ministry of Housing and Urban-Rural Development of China (MOHURD): Beijing, China, 2009.
48. Khankhaje, E.; Kim, T.; Jang, H.; Kim, C.-S.; Kim, J.; Rafieizonooz, M. Properties of Pervious Concrete Incorporating Fly Ash as Partial Replacement of Cement: A Review. *Dev. Built Environ.* **2023**, *14*, 100130. [CrossRef]
49. Jiang, Z.W.; Sun, Z.P.; Wang, P.M. Effects of Some Factors on Properties of Porous Pervious Concrete. *J. Build. Mater.* **2005**, *8*, 513–519.
50. Zhang, C.; Zhang, X.; Hou, J.; Wang, J.; Duan, G. Rheology and Early Microstructure Evolution of Fresh Ultra-High Performance Concrete with Polycarboxylate Superplasticizer. *Case Stud. Constr. Mater.* **2022**, *17*, e01575. [CrossRef]
51. Xiong, B.; Gao, H.; Lu, X.; Tian, B.; Zhang, P.; Chen, B. Influence of Maximum Paste Coating Thickness without Void Clogging on the Pore Characteristics and Seepage Flow of Pervious Concrete. *Constr. Build. Mater.* **2023**, *392*, 131979. [CrossRef]
52. Pereira Da Costa, F.B.; Haselbach, L.M.; Da Silva Filho, L.C.P. Pervious Concrete for Desired Porosity: Influence of w/c Ratio and a Rheology-Modifying Admixture. *Constr. Build. Mater.* **2021**, *268*, 121084. [CrossRef]

53. Luo, Y.; Lv, Y.; Wang, D.; Jiang, Z.; Xue, G. The Influence of Coarse Aggregate Gradation on the Mechanical Properties, Durability, and Plantability of Geopolymer Pervious Concrete. *Constr. Build. Mater.* **2023**, *382*, 131246. [CrossRef]
54. Claudino, G.O.; Rodrigues, G.G.O.; Rohden, A.B.; Mesquita, E.F.T.; Garcez, M.R. Mix Design for Pervious Concrete Based on the Optimization of Cement Paste and Granular Skeleton to Balance Mechanical Strength and Permeability. *Constr. Build. Mater.* **2022**, *347*, 128620. [CrossRef]
55. Yogesh, R.V.; Santha, G.K.; Ganesh, K.S. Synergistic Effect of Aggregate Gradation Band and Cement to Aggregate Ratio on the Performance of Pervious Concrete. *J. Build. Eng*. **2023**, *73*, 106718. [CrossRef]
56. Xie, X.; Zhang, T.; Wang, C.; Yang, Y.; Bogush, A.; Khayrulina, E.; Huang, Z.; Wei, J.; Yu, Q. Mixture Proportion Design of Pervious Concrete Based on the Relationships between Fundamental Properties and Skeleton Structures. *Cem. Concr. Compos.* **2020**, *113*, 103693. [CrossRef]
57. Neithalath, N.; Sumanasooriya, M.S.; Deo, O. Characterizing Pore Volume, Sizes, and Connectivity in Pervious Concretes for Permeability Prediction. *Mater. Charact.* **2010**, *61*, 802–813. [CrossRef]
58. Li, H.; Yang, J.; Yu, X.; Zhang, Y.; Zhang, L. Permeability Prediction of Pervious Concrete Based on Mix Proportions and Pore Characteristics. *Constr. Build. Mater.* **2023**, *395*, 132247. [CrossRef]
59. Chen, X.; Wang, H.; Najm, H.; Venkiteela, G.; Hencken, J. Evaluating Engineering Properties and Environmental Impact of Pervious Concrete with Fly Ash and Slag. *J. Clean. Prod.* **2019**, *237*, 117714. [CrossRef]
60. Kia, A. Freeze-Thaw Durability of Air-Entrained High-Strength Clogging Resistant Permeable Pavements. *Constr. Build. Mater.* **2023**, *400*, 132767. [CrossRef]
61. Mohammed, B.S.; Liew, M.S.; Alaloul, W.S.; Khed, V.C.; Hoong, C.Y.; Adamu, M. Properties of Nano-Silica Modified Pervious Concrete. *Case Stud. Constr. Mater.* **2018**, *8*, 409–422. [CrossRef]
62. Chen, Y.; Wang, K.; Wang, X.; Zhou, W. Strength, Fracture and Fatigue of Pervious Concrete. *Constr. Build. Mater.* **2013**, *42*, 97–104. [CrossRef]
63. Nili, M.; Afroughsabet, V. The Long-Term Compressive Strength and Durability Properties of Silica Fume Fiber-Reinforced Concrete. *Mater. Sci. Eng. A* **2012**, *531*, 107–111. [CrossRef]
64. Zhong, R.; Wille, K. Influence of Matrix and Pore System Characteristics on the Durability of Pervious Concrete. *Constr. Build. Mater.* **2018**, *162*, 132–141. [CrossRef]
65. Monteagudo, S.M.; Moragues, A.; Gálvez, J.C.; Casati, M.J.; Reyes, E. The Degree of Hydration Assessment of Blended Cement Pastes by Differential Thermal and Thermogravimetric Analysis. Morphological Evolution of the Solid Phases. *Thermochim. Acta* **2014**, *592*, 37–51. [CrossRef]
66. Bhattacharya, M.; Harish, K.V. An Integrated Approach for Studying the Hydration of Portland Cement Systems Containing Silica Fume. *Constr. Build. Mater.* **2018**, *188*, 1179–1192. [CrossRef]
67. Hanehara, S.; Tomosawa, F.; Kobayakawa, M.; Hwang, K. Effects of Water/Powder Ratio, Mixing Ratio of Fly Ash, and Curing Temperature on Pozzolanic Reaction of Fly Ash in Cement Paste. *Cem. Concr. Res.* **2001**, *31*, 31–39. [CrossRef]
68. Zeng, Q.; Li, K.; Fen-chong, T.; Dangla, P. Pore Structure Characterization of Cement Pastes Blended with High-Volume Fly-Ash. *Cem. Concr. Res.* **2012**, *42*, 194–204. [CrossRef]
69. *ACI Committee 522; ACI SPEC-522.1-13*; Specification for Pervious Concrete Pavement. American Concrete Institute: Hills, MI, USA, 2013.
70. *CJJ/T 135-2009*; Technical Specification for Pervious Cement Concrete Pavement. Standards Press of China: Beijing, China, 2023.
71. *JC/T 2558-2020*; Pervious Concrete. Standards Press of China: Beijing, China, 2020.